SolarPACES 2022, 28th International Conference on Concentrating Solar Power and Chemical Energy Systems
Measurement Systems, Devices, and Procedures
https://doi.org/10.52825/solarpaces.v1i.715

Published: 02 Feb. 2024

Experimental Methods for Measuring the Efficiency of a Molten Salt Central Receiver

María Fernández-Torrijos[1][https://orcid.org/0000-0001-7834-8240], Cathy Frantz[2][https://orcid.org/0000-0002-3455-3311], Jana Stengler[2][https://orcid.org/0000-0001-6124-8286], Marc Röger[2][https://orcid.org/0000-0003-0618-4253], Tim Schlichting[2][https://orcid.org/0000-0001-7278-1166], and Reiner Buck[2][https://orcid.org/0000-0002-3821-9409]

[1] Departamento de Ingeniería Térmica y de Fluidos, Spain.

[2] Institute of Solar Research, German Aerospace Center, Germany.

Abstract. In this work, two different methods for measuring the efficiency of central receivers are analyzed by the case of the High Performance Molten Salt II Project (HPMS-II): the continuous power-on method, and the semi-analytical method. The main difference between the two methods is the procedure to calculate the thermal losses of the receiver: on the one hand, the continuous power-on method calculates the thermal losses from the measurement of the absorbed power by the molten salt for different measured incident powers on the receiver. Here, it is assumed that the thermal losses are independent of the incident power if the molten salt temperature is kept constant. On the other hand, the semi-analytical method calculates the thermal losses as the sum of convective and radiative losses, calculated directly from the Newton and Stefan-Boltzmann equations by measuring the temperature of the tube surface, the ambient temperature, and the wind speed. Therefore, the calculation of the thermal losses is independent from one method to another. The procedure of applying these methods during the experimental test campaign of the HPMS-II receiver is detailed in this paper. Additionally, an uncertainty analysis of both methods is conducted to determine the uncertainty expected for the receiver efficiency measurements.

Keywords: Uncertainty Analysis, Solar Receiver, Molten Salt, Power-on Method, Efficiency measurement, Solar Salt

1. Introduction

Concentrating solar power (CSP) with thermal energy storage (TES) is one of the most promising renewable energy technologies for dispatchable electricity generation. It increases the flexibility of the electricity system, allowing CSP plants to operate independently or in combination with other renewable energies such as photovoltaics and wind, avoiding the need of fuel backup or massive battery storages. However, these systems are not completely mature, and several challenges must be overcome to reduce the cost and increase the efficiency of the plant. In that sense, the main purpose of the High Performance Molten Salt II (HPMS-II) Project is to demonstrate that a closed-circuit of molten salt permits to increase the maximum operational temperature from 565 ºC to 600 ºC without causing decomposition of the molten salt and minimizing corrosion of the tubes. One of the goals of the project is the measurement of the receiver efficiency, which is defined as the ratio between the power absorbed by the molten salt and the incident solar power onto the receiver.

$$\eta_{rec} = \frac{P_{MS}}{P_{inc}} = \frac{P_{MS}}{\frac{P_{MS}+P_{loss,th}}{\alpha_s}} = \frac{\alpha_s}{1+\frac{P_{loss,th}}{P_{MS}}} \quad (1)$$

where $P_{MS} = \dot{m}\ c_p\ (T_{out} - T_{in})$ is the absorbed power by the molten salt, $P_{loss,th}$ are the thermal losses of the receiver and α_s is the hemispherical absorptance over the solar spectrum of the tubes.

Different methods for measuring the receiver efficiency on industrial-scale receivers can be found in the literature: classical and innovative methods based on the measurement of incident solar power [1-4], a practical method based on direct normal irradiance (DNI) measurement [5], and the power-on method [6] which was successfully applied to Solar-Two plant two decades ago. The power-on method avoids the necessity of measuring the incident power, which in some cases comes along with a high measurement uncertainty.

The power-on method divides the heliostat field in two groups of equal number of heliostats, so that the receiver is operated at full power using the heliostats of both groups, and then at half power using the heliostats of only one group. The molten salt inlet and outlet temperatures remain constant for both full and half power cases, so that the mass flow rate must be adjusted. Under the assumption that the thermal losses are independent of the incident power for steady state conditions with constant molten salt temperature, the thermal losses of the receiver are calculated from the measurement of absorbed power for both full and half incident power. Although this assumption is not completely accurate (primarily due to the marginally elevated surface temperatures at increased flux levels), any inaccuracies associated with it remain comfortably within the measurement's range of uncertainty. Therefore, thermal losses can be considered constant [6]. One of the main disadvantages of the power-on method is that the efficiency can only be measured by means of defocusing half of the heliostat field around solar noon. Therefore, additional effort was required to find and adapt a suitable methodology for this receiver that allows to measure the efficiency without affecting the heliostat field arrangement and control.

In this work, two different methods for measuring the receiver efficiency of the HPMS-II project are presented for the first time: the continuous power-on method, and the semi-analytical method with wall temperature measurements. The procedure to apply these methods during the experimental campaign of testing the receiver of HPMS-II, and also an uncertainty analysis of the receiver efficiency for both methods are detailed in this paper.

2. Continuous power-on method

The proposed continuous power-on method is a variation of the power-on method used in Solar-Two experimental campaign [6], with the difference that in the continuous power-on method it is not necessary to divide the heliostat field in two groups for conducting experiments at full and half incident power. The continuous power-on method can be applied without affecting the heliostat field arrangement and control for nominal operation of the solar tower plant, by means of measuring the ratio between the high and low incident power with the radiometers installed in the HPMS-II receiver. Although the uncertainty of the measured incident power is high, the sensitivity of the uncertainty of the ratio between the high and low incident flux density in the combined receiver efficiency uncertainty calculated from an energy balance is low. The suggested approach is defining different power levels to be reached along the daily tower plant operation, and make pairs of power levels for applying the power-on method. Whereas the power-on method used in Solar -Two experimental campaign consisted in conducting four experiments per day around solar noon (full power from 11.00 to 11:30 and 12:00 to 12:30, and half power from 11:30 to 12:00 and 12:30 to 13:00) to minimize the changing cosine effects of the heliostat field [3], the continuous power-on method proposed in this work uses in the uncertainty analysis as many power levels as feasible for the receiver to reach the steady state, independently of the solar time, which results in lower uncertainty in the determined receiver efficiency. Two advantages of the continuous power-on method are pointed out compared to the conventional power-on method: i) The continuous power-on method can be applied without affecting the heliostat field arrangement and control for nominal operation of the power plant,

ii) The higher number of experimental power levels reduces the receiver efficiency uncertainty significantly (around 2% reduction for an increase of 2 pairs of power levels).

The experimental procedure to apply the continuous power-on method for the HPMS-II receiver is detailed in the following steps:

1. Define the inlet and outlet temperature of the molten salt in the receiver, which must be constant for the different incident power levels reached, as one of the assumptions of this method is to consider that the thermal losses are independent of the incident power provided that the molten salt temperature remains constant.
2. Define the incident power levels to be reached onto the receiver. The heliostat field should be operated to have an incident flux on the receiver as uniform as possible.
   For each power level:
3. Measure the incident heat flux with the eight radiometers installed along the height of the HPMS-II receiver (four radiometers at each side of the receiver).
4. Adjust the mass flow rate until the desired temperature range in the molten salt is achieved in the steady state. The mass flow rate is measured with an ultrasonic flow-meter, and the inlet and outlet temperatures of the molten salt are measured with a total of six N-type thermocouples.

Once the experimental procedure for the desired power levels is done, the receiver efficiency for each power level can be obtained as a function of the measured absorbed power of the molten salt $P_{MS} = \dot{m}\, c_p\, (T_{out} - T_{in})$, the solar absorptance of the receiver α_s, and the thermal losses $P_{loss,th}$ (Eq. 1). To calculate the thermal losses, experiments will be arranged in pairs of power levels *i*, relating one high power level with one low power level. Under the assumption that the thermal losses are independent of the incident power, it is fulfilled that

$$P_{MS,H_i} + P_{loss,th} = R_i(P_{MS,L_i} + P_{loss,th}) \tag{2}$$

where $R_i = \frac{P_{inc,H_i}}{P_{inc,L_i}}$ is the ratio between the high and low incident solar power levels. For *n* number of pairs of power levels, *n* equations that relates the high and low incident heat flux of each pair will be fulfilled. Adding all the equations, the thermal losses for the selected constant temperature of the molten salt are calculated as:

$$P_{loss,th} = \frac{\sum_{i=1}^{n} P_{MS,H_i} - \sum_{i=1}^{n}(P_{MS,L_i} \cdot R_i)}{(\sum_{i=1}^{n} R_i) - n} \tag{3}$$

In fact this is a combinational problem with x steady state experiments conducted at the same salt inlet and outlet temperature for different flux densities and k=2 combinations without repetition and no order, so the number of possible combinations is: n=x!/((x-k)!*k!)

3. Semi-analytical method

The semi-analytical method consists of measuring the temperature distribution over the receiver aperture with an IR camera, the wind speed at receiver height and the ambient temperature, and calculate the radiative and convective thermal losses using the Stefan-Boltzmann and Newton laws

$$P_{loss,th} = \sum_{j}^{n_{pixels}} \left(\varepsilon\, \sigma\, \left(T_{s,j}^4 - T_{\infty}^4\right) + h\, \left(T_{s,j} - T_{\infty}\right) \right) A_p \tag{4}$$

where ε is the hemispherical emittance over the respective IR spectrum of the tubes surface, A_p is the front area (projected area along vertical direction) of each pixel seen by the IR camera, h is the external convective heat transfer coefficient from the external surface of

the tubes to the ambient air, $T_{s,j}$ is the external tube surface temperature for each pixel of the IR camera, and T_∞ is the ambient temperature. It is important to mention that the sum over all surface segments A_p must correspond to the real receiver aperture area, also the infrared camera may not see some regions. Once the thermal losses of the receiver are obtained, the efficiency is calculated by Eq.1.

4. Uncertainty analysis

An uncertainty analysis of both the continuous power-on method and semi-analytical method was conducted using the definitions of JCGM 100:2008 [7]. The receiver efficiency is calculated as a function of the absorbed power by the molten salt $P_{MS} = \dot{m}\, c_p\, (T_{out} - T_{in})$, the solar absorptance of the receiver α_s, and the thermal losses $P_{loss,th}$ (Eq. 1), so the combined uncertainty of the receiver efficiency is calculated as

$$\sigma_\eta = \sqrt{\left(\frac{\partial \eta}{\partial \dot{m}}\right)^2 \sigma_{\dot{m}}^2 + \left(\frac{\partial \eta}{\partial c_p}\right)^2 \sigma_{c_p}^2 + \left(\frac{\partial \eta}{\partial T_{in}}\right)^2 \sigma_T^2 + \left(\frac{\partial \eta}{\partial T_{out}}\right)^2 \sigma_T^2 + \left(\frac{\partial \eta}{\partial P_{loss,th}}\right)^2 \sigma_{P_{loss,th}}^2 + \left(\frac{\partial \eta}{\partial \alpha}\right)^2 \sigma_\alpha^2} \tag{5}$$

where η is the receiver efficiency, $\dot{m}$ is the molten salt flow rate, c_p is the specific heat of the molten salt, T_{in} and T_{out} are the inlet and outlet temperatures, respectively, σ is the standard uncertainty of each parameter. The uncertainty of the temperature measurements is conservatively considered to be the uncertainty of the N-type thermocouples used: $\sigma_T = 2\ K$ (after calibration this uncertainty will probably be lower), the uncertainty of the mass flow rate is taken as the uncertainty of the ultrasonic flowmeter ($\delta_{\dot{m}} = 3\ \%$), the uncertainty of the specific heat is considered to be $\delta_{c_p} = 2\ \%$, the uncertainty of the solar absorptance is taken as the uncertainty of the reflectometer used to measure the tubes absorptivity ($\sigma_\alpha = 2\%$). As the thermal losses are not directly measured, but calculated from Eq. 3 for the continuous power-on method, or Eq. 4 for the semi-analytical method, the combined uncertainty of the thermal losses needs to be determined for each method.

Continuous Power-On method

The combined uncertainty of the thermal losses calculated from Eq. 3 is

$$\sigma_{P_{loss,th}} = \sqrt{\begin{aligned}&\sum_{i=1}^{n}\left(\frac{\partial P_{loss,th}}{\partial \dot{m}_{H_i}}\sigma_{\dot{m}_{H_i}}\right)^2 + \sum_{i=1}^{n}\left(\frac{\partial P_{loss,th}}{\partial \dot{m}_{L_i}}\sigma_{\dot{m}_{L_i}}\right)^2 + \sum_{i=1}^{n}\left(\frac{\partial P_{loss,th}}{\partial c_{p_{H_i}}}\sigma_{c_{p_{H_i}}}\right)^2 + \sum_{i=1}^{n}\left(\frac{\partial P_{loss,th}}{\partial c_{p_{L_i}}}\sigma_{c_{p_{L_i}}}\right)^2 + \\ &\sum_{i=1}^{n}\left(\frac{\partial P_{loss,th}}{\partial T_{in,H_i}}\sigma_T\right)^2 + \sum_{i=1}^{n}\left(\frac{\partial P_{loss,th}}{\partial T_{out,H_i}}\sigma_T\right)^2 + \sum_{i=1}^{n}\left(\frac{\partial P_{loss,th}}{\partial T_{in,L_i}}\sigma_T\right)^2 + \sum_{i=1}^{n}\left(\frac{\partial P_{loss,th}}{\partial T_{out,L_i}}\sigma_T\right)^2 + \sum_{i=1}^{n}\left(\frac{\partial P_{loss,th}}{\partial R_i}\sigma_{R_i}\right)^2\end{aligned}} \tag{6}$$

where σ_R is the standard uncertainty of the radiometers used in the receiver of HPMS-II project. The Gardon gauge type radiometers installed in the receiver, which have an accuracy of ±3%, were previously calibrated against a Kendall-type sensor with an accuracy of 0.3%, so the final uncertainty of the Gardon gauge radiometers after the calibration was 0.6% respective to the Kendall-type.

Semi-analytical method

The combined uncertainty of the thermal losses calculated from Eq. 4 is

$$\sigma_{P_{loss,th}} = \sqrt{\left(\frac{\partial P_{loss,th}}{\partial \varepsilon}\right)^2 \sigma_\varepsilon^2 + \sum_{j=1}^{n_p}\left(\frac{\partial P_{loss,th}}{\partial T_{s,j}}\,\sigma_{T_s}\right)^2 + \left(\frac{\partial P_{loss,th}}{\partial T_\infty}\right)^2 \sigma_{T_\infty}^2 + \left(\frac{\partial P_{loss,th}}{\partial h}\right)^2 \sigma_h^2 + \left(\frac{\partial P_{loss,th}}{\partial A_p}\right)^2 \sigma_{A_p}^2} \quad (7)$$

The uncertainty of the thermal emittance is taken as the uncertainty of the reflectometer used to measure the tubes absorptivity ($\sigma_\varepsilon = 2\%$), the uncertainty of the ambient temperature is the uncertainty of the thermocouple ($\sigma_{T_\infty} = 2\ K$), the uncertainty of the pixel area is considered to be $\delta_{A_p} = 2\%$, and the uncertainty of the heat transfer coefficient to ambient was selected to be $\delta_h = 100\%$, as it is obtained by means of experimental correlations for slightly different receiver geometries [8,9,10]. Regarding the surface temperature measured with the IR camera, a conservative uncertainty value of $\sigma_{T_s} = 20\ K$ was selected as the measurement is influenced by unknown parameters as the tube surface thermal emittance or the atmospheric transmissivity.

5. Case study: HPMS-II receiver

For conducting the uncertainty analysis of both continuous power-on method and semi-analytical method, real experimental measurements are needed. However, the experimental campaign to test the HPMS-II receiver is not finished yet, so that analytical data that simulates the measurements that will be obtained during the experimental test receiver is used in the uncertainty analysis of both methods. For this purpose, a simplified 1D numerical model that simulates the thermal behavior of the receiver was developed to obtain the data necessary to conduct the uncertainty analysis, that is the mass flow rate in the receiver, the inlet and outlet temperatures, and the front surface temperature of the tubes. The energy equation applied to the tube wall is

$$\alpha q_{inc}''\, d_o \Delta x = h_o\,(T_w - T_\infty) d_o \Delta x + \varepsilon\,\sigma\left({T_w}^4 - {T_\infty}^4\right) d_o\,\Delta x + U\pi\frac{d_o}{2}\Delta x (T_w - T_\infty) \quad (8)$$

and the energy equation applied to the molten salt flow:

$$\dot{m} c_p (T_{out} - T_{in}) = U\pi\frac{d_o}{2}\,\Delta x (T_w - 0.5(T_{in} + T_{out})) \quad (9)$$

where $U = \left(\frac{d_o}{h_i d_i} + d_o\frac{\ln\left(\frac{d_o}{d_i}\right)}{2\,k}\right)^{-1}$ is the overall heat transfer coefficient from the molten salt flow to the outer surface of the tube. The Petukhov's correlation [11] was used to estimate the heat transfer coefficient from the molten salt to the internal surface of the tube for Reynolds numbers between $2{\cdot}10^4$-$2{\cdot}10^5$. The main parameters used in the simulations of the thermal behavior of the receiver to obtain the data needed for the evaluation of both continuous power-on method and semi-analytical method are summarized in Table 1.

Table 1. Parameters used in the 1D model simulation of the thermal behavior of the receiver.

Geometry features	
External diameter, d_o (m)	0.0368
Tubes per panel, N_t (-)	2
Number of panels, N_p (-)	8
Length, L (m)	2.2
Aperture area, A (m2)	1.295
Tube wall thermal and optical features	
Thermal conductivity DMV 310N, k (W/(mK))	21.5
Thermal Emittance Pyromark, ε (-)	0.8
Solar Absorptance Pyromark, α (-)	0.93
Ambient conditions	
Heat transfer coefficient to ambient, h (W/(m²K))	8.5
Ambient temperature, T_∞ (ºC)	10
Operational constraints	
Mass flow rate, m (kg/s)	3.2-12.8
Molten salt temperature, T_{MS} (ºC)	290-600
Maximum tube temperature, $T_{w,max}$ (ºC)	650
Maximum film temperature, $T_{film,\ max}$ (ºC)	620
Mean incident heat flux, q_{inc}'' (kW/m²)	150-600

6. Results and discussion

In this work, the influence of the molten salt temperature on the receiver efficiency uncertainty obtained with both continuous power-on method and semi-analytical method is analyzed. Therefore, two cases with the minimum and maximum molten salt inlet temperatures (290 ºC and 550 ºC, respectively) are considered in this study. As it is explained above, for applying the continuous power-on method, it is necessary to keep both the molten salt inlet and outlet temperatures constant. Different simulations are conducted to obtain the mass flow rate necessary to obtain a certain molten salt temperature difference between the inlet and the outlet of the receiver, given the incident heat flux and the inlet temperature. Figure 1 shows the results of the mass flow rate as a function of the incident power for different preestablished temperature differences along the receiver, for an inlet temperature of 290 ºC (a) and 550 ºC (b). As shown, lower mass flow rates are required to reach a higher temperature difference in the receiver, given a fixed incident heat flux. Besides, the mass flow rate needs to be increased when the incident heat flux increases to keep the temperature difference along the receiver constant.

Regarding the continuous power-on method, a preliminary study was conducted to analyze the influence of the temperature difference along the receiver and the ratio between the high and low incident power tests on the receiver efficiency. The receiver efficiency uncertainty strongly decreases with higher temperature differences along the receiver up to a value of approximately 50 ºC, where the influence of the temperature range on the HPMS-II receiver efficiency uncertainty gets insignificant [12]. On the other hand, lower uncertainty values were obtained for higher ratios between the high and low incident power.

Therefore, the constant temperature range selected for analyzing the continuous power-on method was the temperature range higher than 50 ºC that provides a higher range of possible incident powers, i.e., ΔT = 50 ºC for T_{in} = 290 ºC and ΔT = 40 ºC for T_{in} = 550 ºC.

Notice that for T_{in} = 550 ºC, the constraints of the maximum film and wall temperature do not allow to have higher temperature difference than 40 ºC on the receiver.

To select the ratio between the high and low incident power, a compromise must be fulfilled between having the highest ratio that allows to have the highest number of different pairs of power levels. For this study, a ratio of 2 (the higher incident power is twice the lower incident power) is selected for conducting the uncertainty analysis.

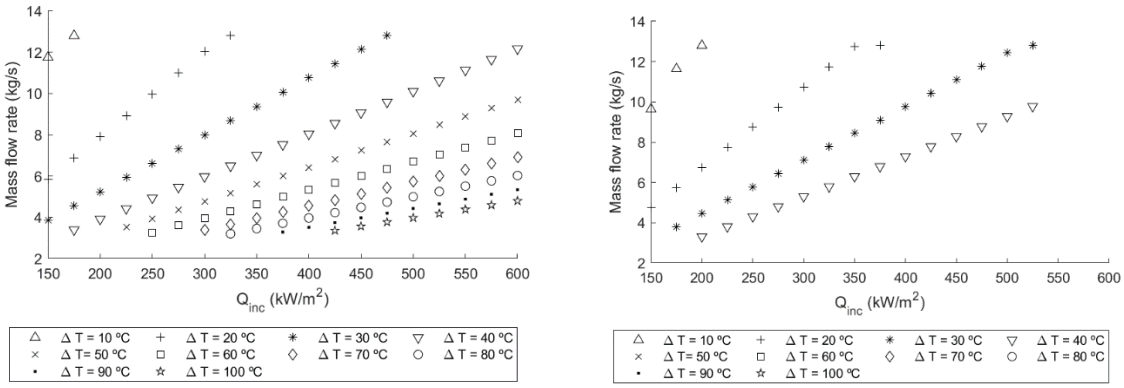

Figure 1. Mass flow rate as a function of incident heat flux for different desired temperature ranges along the receiver. a) Inlet temperature of 290 ºC. b) Inlet temperature of 550 ºC.

Figure 2 shows the efficiency of the HPMS-II receiver as a function of the incident heat flux calculated with the continuous power-on method. The error bar represents the expanded uncertainty with 95% confidence level (k=2) of the receiver efficiency for each incident heat flux, which was around was around 8-20%. It was found that the efficiency uncertainty is mainly dominated by the uncertainty of the thermal losses which have a high range of uncertainty being between 100 and 200%. The thermal loss uncertainty is mainly influenced by the uncertainties of the mass flow rate and inlet and outlet temperatures of the molten salt. However, as the thermal losses are relatively low compared to the absorbed power, their sensitivity on the overall efficiency uncertainty is low. Moreover, Figure 2 shows that the combined uncertainty of the efficiency increases for lower incident powers, as the derivative of the efficiency with respect to thermal losses, which is the predominant parameter in Eq. 5, increases for lower mass flow rates typical of low incident powers.

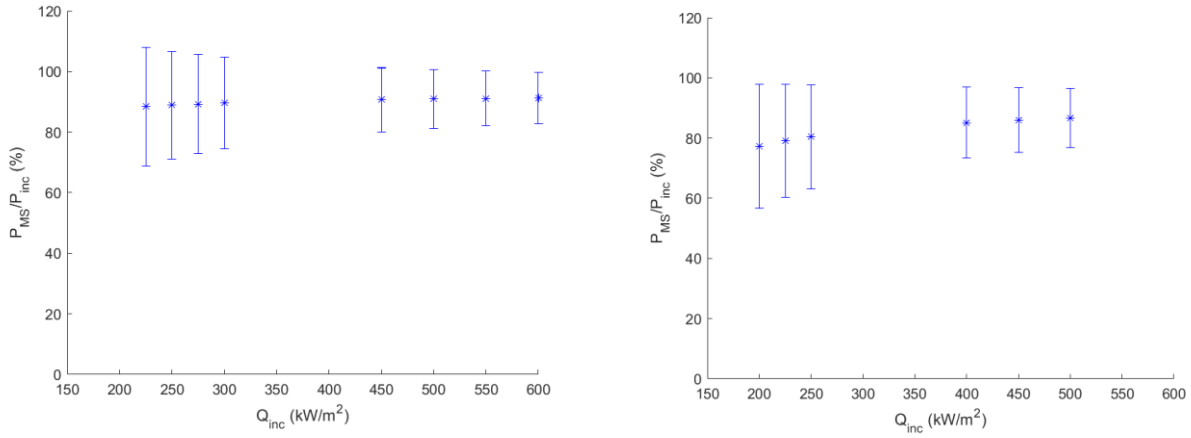

Figure 2. Receiver efficiency calculated with the continuous power-on method for a ratio between high and low incident powers of 2 for a) T_{in} = 290 ºC and T_{out} = 340 ºC, b) T_{in} = 550 ºC and T_{out} = 590 ºC. Error bars show the expanded uncertainty of the efficiency measurement.

Figure 3 shows the efficiency of the study of the HPMS-II receiver as a function of the incident heat flux calculated with the semi-analytical method. The error bar represents the expanded uncertainty with 95% confidence level (k=2) of the receiver efficiency for each incident heat flux. As shown, the expanded uncertainty of the receiver efficiency was around 4-6% for the semi-analytical method, which is lower than the uncertainty obtained with the continuous power-on method, as the uncertainty of the thermal losses was much lower for the semi-analytical method (20-30%) compared to the thermal loss uncertainty obtained with the continuous power-on method (100-200%). Therefore, the efficiency uncertainty obtained with the semi-analytical method is mainly dominated by the uncertainty of the absorptivity of the tubes, and its value remains nearly constant for the different incident powers.

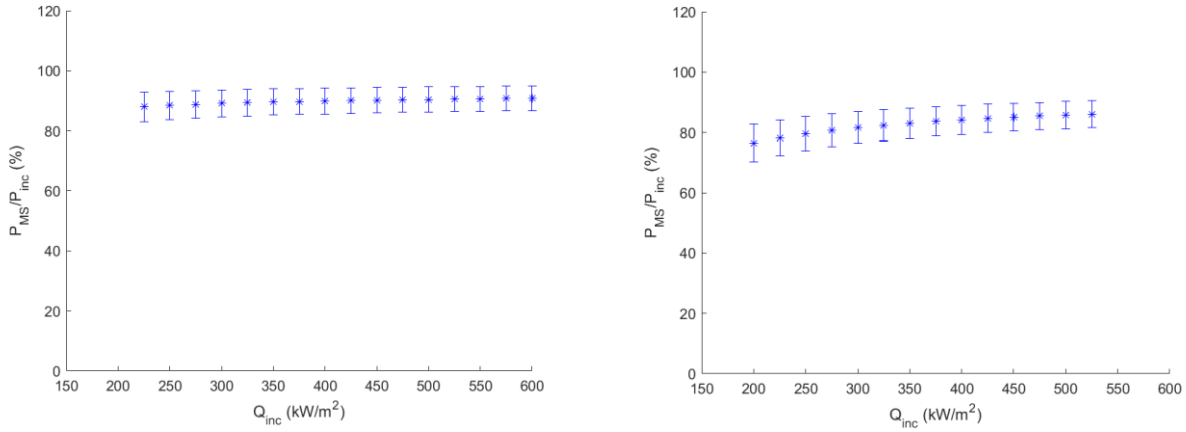

Figure 3. Receiver efficiency calculated with the semi-analytical method for a) T_{in} = 290 ºC and T_{out} = 340 ºC, b) T_{in} = 550 ºC and T_{out} = 590 ºC. Error bars show the expanded uncertainty of the efficiency measurement.

The results of this simulation study have to be confirmed with real HPMS-II measurement data. This work will be done, once the receiver tests have been concluded.

7. Conclusion

In this work, two different methods (continuous power-on method and semi-analytical method) for measuring the receiver efficiency of the High Performance Molten Salt II Project are proposed as novel methods to obtain the efficiency of molten salt receivers at demo scale. The main difference between the two methods is the procedure to calculate the thermal losses of the receiver: on the one hand, the continuous power-on method calculates the thermal losses from the measurement of the absorbed power by the molten salt for different measured incident power levels on the receiver; on the other hand, the semi-analytical method estimates the thermal losses as the sum of convective and radiative losses, calculated directly from the Newton and Stefan-Boltzmann equations by measuring the temperature of the tube surface. Therefore, the calculation of the thermal losses is independent from one method to another.

To study the suitability of applying these methods in the experimental campaign of testing the receiver of the HPMS-II project, an uncertainty analysis of the receiver efficiency is conducted. For studying the influence of the molten salt temperature and incident power on the receiver efficiency uncertainty, different cases with the minimum and maximum molten salt inlet temperatures (290 ºC and 550 ºC, respectively) and minimum and maximum average incident heat flux (from 150 to 600 kW/m^2) are considered for conducting the uncertainty analysis. The results of the study show that the expanded uncertainty with 95% confidence level of the receiver efficiency is around 8-20% for the continuous power-on method, and 4-6% for the semi-analytical method. The lower receiver efficiency uncertainty for the semi-analytical method is due to the lower uncertainty of the thermal losses obtained with the semi-analytical

method compared to that obtained with the continuous power-on method. Since the uncertainty of the receiver efficiency is considered acceptable, both continuous power-on method and semi-analytical method will be performed during the experimental test campaign of the HPMS-II receiver. As the calculation of the thermal losses is independent from one method to another, the comparison of the receiver efficiency results obtained with both methods will provide useful information about the correctness of the efficiency measurements.

Data availability statement

A Matlab code was used to generate the data presented in this paper. The data obtained is presented in graphics in the paper.

Author contributions

M. Fernandez-Torrijos: Conceptualization, Methodology, Formal Analysis, Validation, Data curation, Writing - original draft, Writing - review & editing. **C. Frantz:** Supervision, Conceptualization, Methodology, Validation, Writing - review & editing, **J. Stengler:** Supervision, Review & editing, **M. Röger:** Supervision, Conceptualization, Writing - review & editing, **T. Schlichting:** Supervision, Conceptualization, Writing - review & editing, **R. Buck:** Supervision

Competing interests

The authors declare no competing interests.

Funding

This work has been funded by the Spanish Ministry of Science, Innovation and Universities under the scholarship “Estancias de movilidad en el extranjero José Castillejo para jóvenes doctores” (CAS21_00519) and the fellowship “Programa de apoyo a la realización de proyectos interdisciplinares de I + D para jóvenes investigadores de la Universidad Carlos III de Madrid 2021-2022” under the project ROTORNEA-CM-UC3M funded on the frame of “Convenio Plurianual Comunidad de Madrid-Universidad Carlos III de Madrid 2019-2022”.

This work has been funded by the “German Federal Ministry for Economic Affairs and Energy” (0324327A) as well as by the “Ministerium für Wirtschaft, Innovation, Digitalisierung und Energie des Landes Nordrhein-Westfalen” (PRO 0071).

References

1. M. Röger, P. Herrmann, S. Ulmer, M. Ebert, C. Prahl, F. Göhring, “Techniques to Measure Solar Flux Density Distribution On Large-Scale Receivers”. J. Sol. Energy Eng. vol. 136, no. 3, pp. 031013 (10 pages), 2014, https://doi.org/10.1115/1.4027261
2. M. Offergeld, M. Röger, H. Stadler, P. Gorzalka, B. Hoffschmidt, “Flux Density Measurement for Industrial-Scale Solar Power Towers Using the Reflection of the Absorber”. AIP Conference Proceedings, vol. 2126, pp. 110002, 2019, doi: https://doi.org/10.1063/1.5117617
3. C. Raeder, M. Offergeld, A. Lademann, D. Meyer, J. Zöller, M. Glinka, M. Röger, A. Kämpgen, J. Escamilla, “Proof of Concept: Real-time Flux Density Monitoring System on external Tube Receivers for Optimized Solar Field Operation”, SolarPACES conference 2021, online, to be published in AIP 2022

4. M. Ebert, D. Benitez, M. Röger, R. Korzynietz, J.A. Brioso, “Efficiency determination of tubular solar receivers in central receiver systems”, Solar Energy, vol. 139, pp. 179–189, 2016, doi: http://dx.doi.org/10.1016/j.solener.2016.08.047
5. G. Xiao, J. Zeng, J. Nie, “A practical method to evaluate the thermal efficiency of solar molten salt receivers”. Applied Thermal Engineering, vol. 190, pp. 116787, 2021, doi: https://doi.org/10.1016/j.applthermaleng.2021.116787
6. J. Pacheco et al., “Final Test and Evaluation Results from the Solar Two Project”, SAND2002-0120, Albuquerque.
7. Evaluation of measurement data- guide to the expression of uncertainty in measurement, JCGM 100-2008.
8. D. L. Siebers, R. F. Moffatt, R. G. Schwind, “Experimental, Variable Properties Natural Convection From a Large, Vertical, Flat Surface”. J. Heat Transfer, vol. 107, pp. 124-132, 1985, doi: https://doi.org/10.1115/1.3247367
9. D.L. Siebers, J.S. Kraabel, “Estimating Convective Energy Losses from Solar Central Receivers”, Livermore, 1984, doi: https://doi.org/10.2172/6906848
10. R.F. Bohem, “Review of Thermal Loss Evaluations of Solar Central Receivers”, SAND85-8019, Albuquerque, 1986.
11. B.S. Petukhov, “Heat transfer and friction in turbulent pipe flow with variable physical properties“, Advances in heat transfer 6 (1970) 503-564.
12. C. Frantz, M. Ebert, B. Schlögl-Knothe, M. Binder, C. Schuhbauer, “Experimental Receiver Setup of a High Performance Molten Salt Test Receiver System”, SolarPACES conference 2021, online, to be published in AIP 2022